

# A Numerical and Experimental Analysis of the Performance of a Combined Solar Unit for Air Conditioning and Water Desalination

Zied Guidara, Alexander Morgenstern, Aref Younes Maalej

**Abstract**—In this paper, a desiccant solar unit for air conditioning and desalination is presented first. Secondly, a dynamic modelling study of the desiccant wheel is developed. After that, a simulation study and an experimental investigation of the behaviour of desiccant wheel are developed. The experimental investigation is done in the chamber of commerce in Freiburg-Germany. Indeed, the variations of calculated and measured temperatures and specific humidity of dehumidified and rejected air are presented where a good agreement is found when comparing the model predictions with experimental data under the considered range of operating conditions. Finally, the study of the compartments of desalination and water condensation shows that the unit can produce an acceptable quantity of water at the same time of the air conditioning operation.

**Keywords**—Air conditioning, desalination, condensation, design, desiccant wheel.

## I. INTRODUCTION

PROVIDING conditioned air and fresh water is a necessity in daily life. However, conventional units, which are used to satisfy this need, have a negative impact on the environment and consume an important quantity of electricity. So solving these problems should be realized without breaking the international commitments relative to the environmental protection. Indeed, these commitments mainly intend to reduce CO<sub>2</sub> emissions, avoid the use of harmful gases to the ozone layer and to the greenhouse effect used especially in the conventional air conditioners. In this context, desiccant units of air conditioning present a promising solution for air-conditioning, in terms of environmental protection and energy saving. In addition, desiccant dehumidification is advantageous in handling latent heat, easy to be regenerated using low-grade energy, such as solar energy [1]. Furthermore, with conventional units of air conditioning, the dehumidification of the air is done through a cooling operation under dew point temperature [2]. Thus, the air is too cold to be used as direct supply air to the conditioned space and has to be heated up again. This operation can be characterized as an energy consuming procedure [3] and in some cases; it cannot

ensure the achievement of temperature and humidity levels required by the user [4]. For temperate climates, standards configurations are typically employed. However, as far as the climates in the Mediterranean countries are concerned, other configurations of desiccant processes have to be implemented [5], [6]. In fact, a block of cooling in these configurations is generally installed, before or after dehumidifying the air. The cooling, on the other hand, is obtained by cooling coils that are fed by cold water which is produced by machines with sorption technique or conventional refrigerated machines.

G. Panaras et al. [7] showed that the desiccant wheel is a basic element of desiccant air-conditioning systems, responsible for the dehumidification of the air. In addition, solar powered desalination systems, which are based on humidification and dehumidification principles, are becoming more popular throughout the world.

In this research work, a design of a desiccant solar unit for air conditioning and desalination is presented. The main components are a desiccant wheel to dehumidify the air, solar collector to produce hot water for regeneration, humidifiers for humidification and a combination of heat exchangers-humidifiers to ensure the cooling of the air without the use of machines with sorption technique or conventional refrigerated machines. In addition, a desalination compartment and a condensation water compartment are used in this unit. Indeed, the functioning of the desalination one is based on the dehumidification-humidification process and the condensation water compartment is based on the cooling under the dew point temperature of the rejected air. Furthermore, a modelling study and an experimental investigation of the functioning of the desiccant wheel are presented. This is done in order to validate the developed model which will be used after that in the numerical study of the desalination compartment and the condensation water compartment.

The content of this paper is organized as follows. Section II is dedicated to the design of the new developed unit. In Section III, the functioning of the unit is described. Section IV presents a modelling study of the desiccant wheel. In Section V, a simulation study and an experimental investigation of the functioning of the desiccant wheel are presented. In Section VI, a numerical study concerning the compartments of desalination and water condensation is developed. Finally, Section VII presents the main conclusion of this work.

## II. DESIGN OF THE SOLAR AIR CONDITIONING UNIT

The design of the desiccant solar unit is presented in Fig. 1.

Zied Guidara and Aref Younes are with the Laboratory of Electro-Mechanic Systems (LASEM), National School of Engineers of Sfax (ENIS), University of Sfax (US), B.P. 1173, Road Soukra km 3.5, 3038 Sfax, Tunisia (e-mail: ziedguidara@yahoo.fr, aref.maalej1@gmail.com).

Alexander Morgenstern is with the Division Thermal Systems and Buildings, Fraunhofer-Institut für Solare Energiesysteme ISE Heidenhofstraße 2, 79110 Freiburg, Germany (e-mail: alexander.morgenstern@ise.fraunhofer.de).

Compared with standard unit for air conditioning, two compartments are added. Indeed, the first one is responsible of the pre-cooling of the ambient air and the desalination of the salty underground cold water. The second one is dedicated to

the water condensation. The first compartment is mainly composed by: a humidifier HUM4 and a heat exchanger HEX4. The second compartment is mainly composed by a heat exchanger HEX.

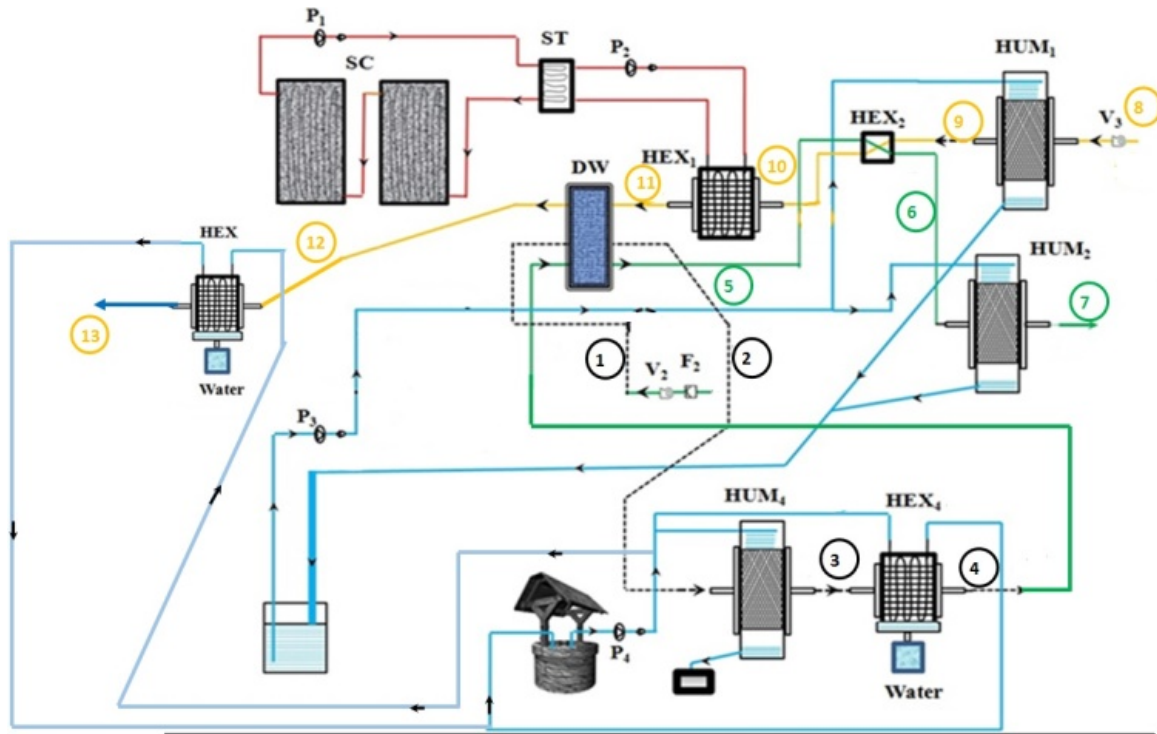


Fig. 1 Design of the desiccant solar unit

### III. DESCRIPTION OF THE FUNCTIONING OF THE UNIT

Three main cycles of functioning are distinguished for this unit. The principle of functioning can be described as follows:

#### \*Desalination Cycle:

The ambient air is dehumidified and heated (from 1, to 2) by passing through a desiccant wheel DW. Then, the dehumidified air is humidified and cooled (from 2 to 3) close to the saturation in the humidifier HUM4 by the use of salty underground water. Later on, this cooled and humidified air passes through a water/air heat exchanger HEX4 to be dehumidified by cooling under its dew point temperature (from 3 to 4). As a consequence a quantity of pure water is obtained by condensation at the exit of the heat exchanger water/air HEX4.

#### \*Air Conditioning Cycle:

The cold and saturated air (point 4) is dehumidified and heated (from 4 to 5) by passing through a desiccant wheel DW. Later on, the dehumidified air is pre-cooled (from 5 to 6) in an air/air heat exchanger HEX2 by the air that returns from the space conditioned, humidified and cooled (from 8 to 9) close to the saturation in the humidifier HUM1. Furthermore, the air is cooled (from 6 to 7) to the desired temperature and humidity in the humidifier HUM2 corresponding to the state of human comfort.

Concerning the regeneration, the air that returns from the

conditioned space humidified and cooled (from 8 to 9) is pre-heated (from 9 to 10) by passing through an air/air heat exchanger HEX2. Furthermore, the pre-heated air is heated (from 10 to 11) by passing through a water/air heat exchanger HEX1 where the hot water is produced by the solar energy from flat plate solar collectors and a storage tank. Then, this hot air passes through the hygroscopic wheel to ensure its regeneration (from 11 to 12).

#### \*Water Condensation Cycle:

The rejected air (point 12) is relatively humid and hot. This air passes through a water/air heat exchanger HEX to be cooled under its dew point temperature (from 12 to 13). As a consequence, a quantity of pure water is obtained by condensation.

### IV. MODELLING STUDY

The modelling of the desiccant wheel is based on mass and thermal balances for the airflow and the desiccant. The desiccant wheel is divided in two parts, the first one is for the dehumidification and the second is for the regeneration (Fig. 2). The used desiccant is the silica gel.

To develop the mathematical model, these assumptions are followed:

- hysteresis in the sorption isotherm for desiccant coating is neglected and the heat of sorption (adsorption/desorption)

- is assumed constant,
- the canals are adiabatic, impermeable, with the same material and identical,
- the airflow is uni-directional,
- the thermodynamic properties of dry air, vapour, and desiccant are uniform and constants,
- the heat and mass coefficients between the air stream and the desiccant wall are constant along the channel.

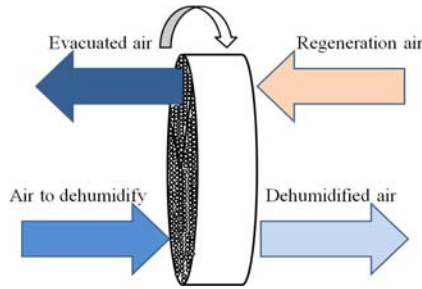


Fig. 2 The studied desiccant wheel

Thus, the mathematical model of the desiccant wheel is written as [8]:

$$A \cdot \rho_a \cdot C_{pa} \cdot V \cdot L \cdot \frac{\partial T}{\partial x} + A \cdot \rho_a \cdot C_{pa} \cdot L \cdot \frac{\partial T}{\partial t} = h \cdot A_{lat} \cdot (T_p - T) \quad (1)$$

$$A \cdot \rho_a \cdot V \cdot L \cdot \frac{\partial \omega}{\partial x} + A \cdot \rho_a \cdot L \cdot \frac{\partial \omega}{\partial t} = h_m \cdot A_{lat} \cdot (\omega_p - \omega) \quad (2)$$

$$A_d \cdot Q_{ads} \cdot \rho_d \cdot L \cdot \frac{\partial W}{\partial t} = h \cdot A_{lat} \cdot (T_p - T) + A_d \cdot \rho_d \cdot C_{pd} \cdot L \cdot \frac{\partial T_p}{\partial t} \quad (3)$$

$$A_d \cdot \rho_d \cdot L \cdot \frac{\partial W}{\partial t} = h_m \cdot A_{lat} \cdot (\omega - \omega_p) \quad (4)$$

$$\omega_p = \frac{0.62188 \cdot \varphi_p}{\frac{p_{atm}}{p_{ws}} - \varphi_p} \quad (5)$$

$$p_{ws} = \exp\left(23.196 - \frac{3816.44}{T_p - 46.13}\right) \quad (6)$$

$$\varphi_p = 0.0078 - 0.05759 \cdot W + 24.16554 \cdot W^2 - 124.78 \cdot W^3 + 204.226 \cdot W^4 \quad (7)$$

## V. SIMULATION STUDY AND EXPERIMENTAL INVESTIGATION

The numerical simulation is done by use of an explicit finite differential method. The experimental investigation is done in the chamber of commerce in Freiburg-Germany. The used desiccant wheel is DehuTech DT 15-1720. Transmitters' series FTW65 are used to measure relative humidity and temperature.

The working conditions, the thermodynamic properties, and the geometrical size are listed in Table I.

TABLE I  
 THE WORKING CONDITIONS, THE THERMODYNAMIC PROPERTIES, AND THE GEOMETRICAL SIZE

| Parameter                               | Value                | Unit                   |
|---|----------------------|------------------------|
| Density of the air $\rho_a$             | 1.016                | (kg/m <sup>3</sup> )   |
| Specific heat of the air $C_{pa}$       | 1009                 | (J/kg.K)               |
| Length of one canal $L$                 | 0.3                  | (m)                    |
| Heat transfer coefficient $h$           | 50                   | (W/m <sup>2</sup> .K)  |
| Mass transfer coefficient $h_m$         | 0.04955              | (kg/m <sup>2</sup> .s) |
| Adsorption heat $Q_{ads}$               | 2300.10 <sup>3</sup> | (J/kg)                 |
| Volume flow of the dehumidified air     | 7500                 | m <sup>3</sup> /h      |
| Volume flow of the regenerated air      | 2500                 | m <sup>3</sup> /h      |
| Density of the desiccant $\rho_d$       | 1129                 | (kg/m <sup>3</sup> )   |
| Specific heat of the desiccant $C_{pd}$ | 921                  | (J/kg.K)               |
| Space step $\Delta x$                   | 0.01                 | (m)                    |
| Time step $\Delta t$                    | 0.1                  | (s)                    |
| Radius of the hygroscopic wheel $R$     | 0.86                 | (m)                    |

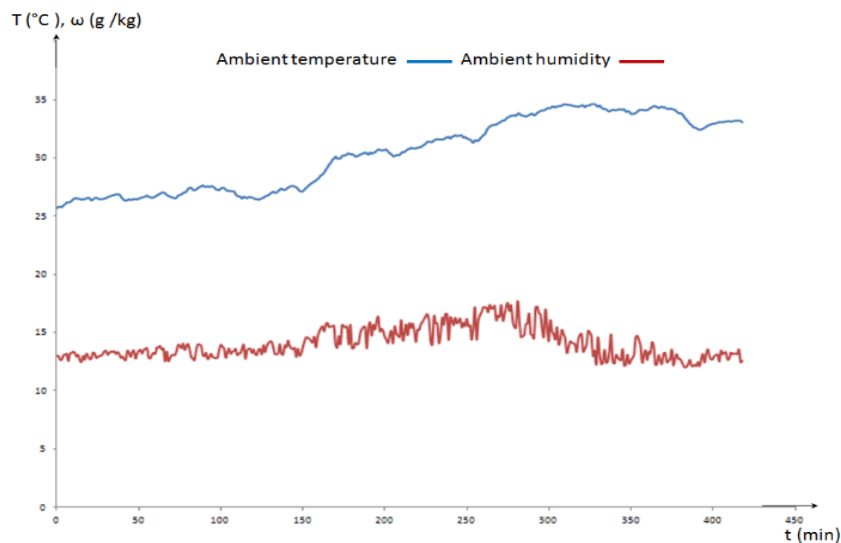


Fig. 3 Variations of ambient air temperature and ambient humidity ratio

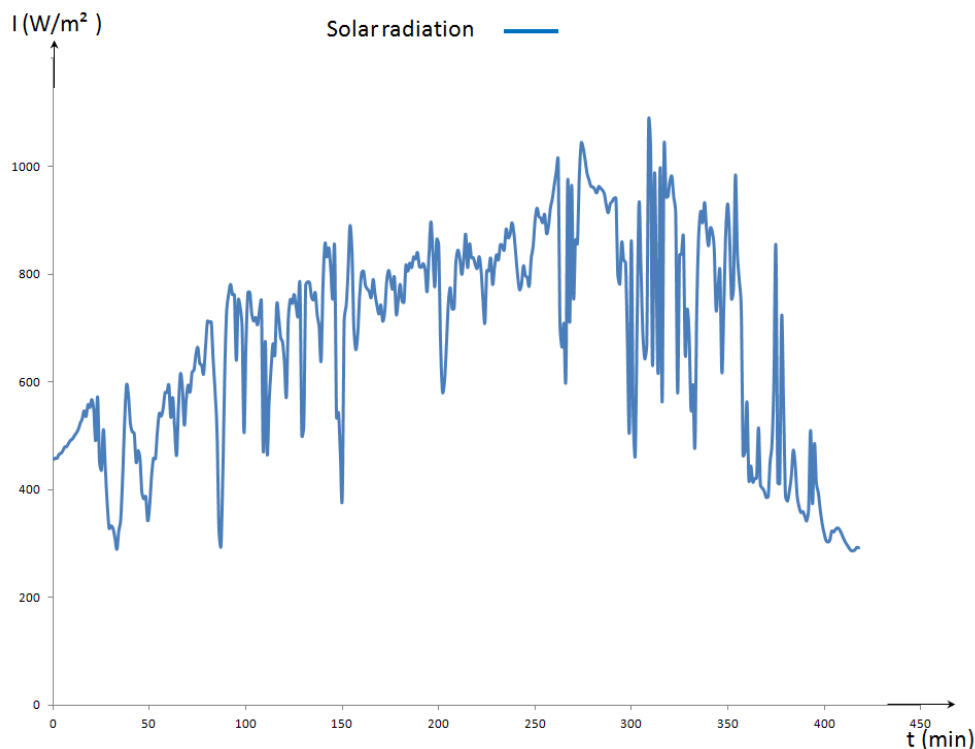


Fig. 4 Variations of solar radiation

*A. Variation of Inlet Parameters for the Dehumidification and Regeneration Processes*

The presented data are measured for a typical day in June from 9:00 to 15:53 h every minute. The variations of ambient air temperature and ambient humidity ratio are presented in Fig. 3. The results show that the minimum value of the ambient air temperature is equal to 25.7°C at 9 am and the maximum value is equal to 34.4°C at 2pm 25min.

The variation of solar radiation is presented in Fig. 4. The results show that the maximum value of the solar radiation exceeds 1000 W/m<sup>2</sup> 8 times and the minimum value is equal to 294 W/m<sup>2</sup> at 15:53 h.

The variation of regeneration temperature is presented in Fig. 5. The results show that the minimum value of the regeneration air temperature is equal to 37°C at 9 am and the maximum value is equal to 70°C at 1pm 48min.

Note that 18 points are considered to develop the simulation study as it is mentioned in Table II. These values correspond to the measured values. Indeed, these 18 points are the inlet parameters for the desiccant wheel for the dehumidification and regeneration processes.

TABLE II  
 VALUES OF THE USED 18 POINTS FOR THE SIMULATION OF THE DESICCANT WHEEL

| Parameter | Ambient temperature (°C) | Ambient humidity (g/kg) | Regeneration temperature (°C) | Time (min) |
|-----------|--------------------------|-------------------------|-------------------------------|------------|
| Point 1   | 25.7                     | 12.96                   | 37.3                          | 0          |
| Point 2   | 26.5                     | 12.91                   | 41.2                          | 25         |
| Point 3   | 26.5                     | 13.41                   | 39.4                          | 50         |
| Point 4   | 26.8                     | 13.87                   | 45.9                          | 75         |
| Point 5   | 27.3                     | 13.94                   | 50.3                          | 100        |
| Point 6   | 26.5                     | 13.13                   | 51.2                          | 125        |
| Point 7   | 27.1                     | 13.7                    | 54.3                          | 150        |
| Point 8   | 30.2                     | 15.54                   | 56.5                          | 175        |
| Point 9   | 30.6                     | 14.63                   | 60.2                          | 200        |
| Point 10  | 31.2                     | 16.42                   | 60                            | 225        |
| Point 11  | 31.6                     | 16.18                   | 61.5                          | 250        |
| Point 12  | 33.4                     | 17.55                   | 65.9                          | 275        |
| Point 13  | 34.2                     | 14.25                   | 63.8                          | 300        |
| Point 14  | 34.4                     | 15                      | 66.7                          | 325        |
| Point 15  | 33.7                     | 12.56                   | 63.4                          | 350        |
| Point 16  | 34.1                     | 13.53                   | 48.4                          | 375        |
| Point 17  | 32.9                     | 12.72                   | 46.5                          | 400        |
| Point 18  | 33.15                    | 13.16                   | 42.7                          | 413        |

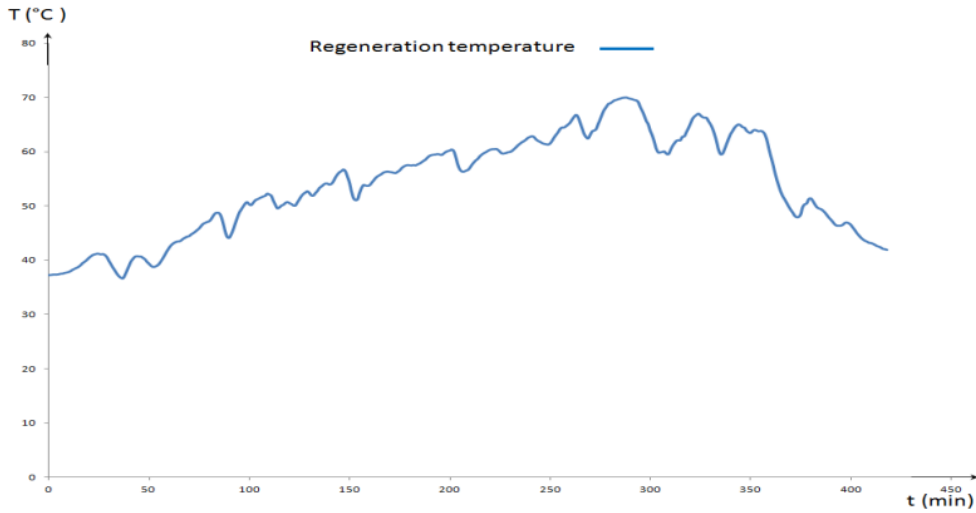


Fig. 5 Variations of regeneration temperature

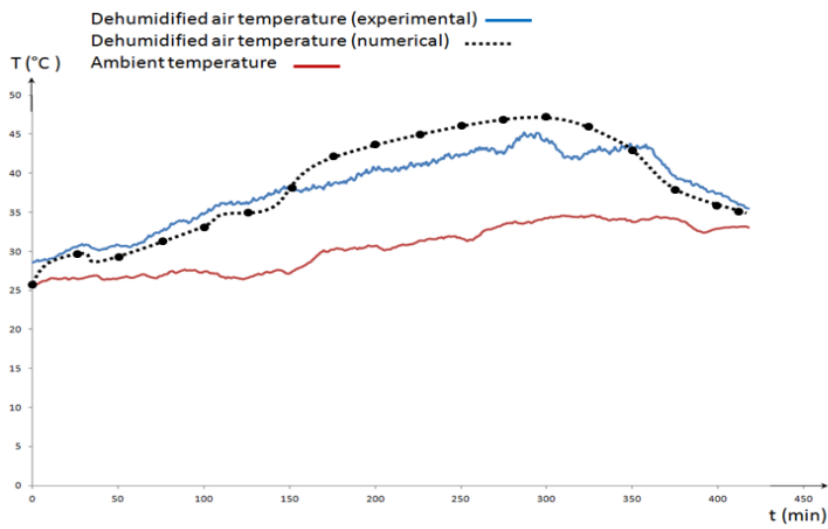


Fig. 6 Variation of numerical and experimental dehumidified air temperature

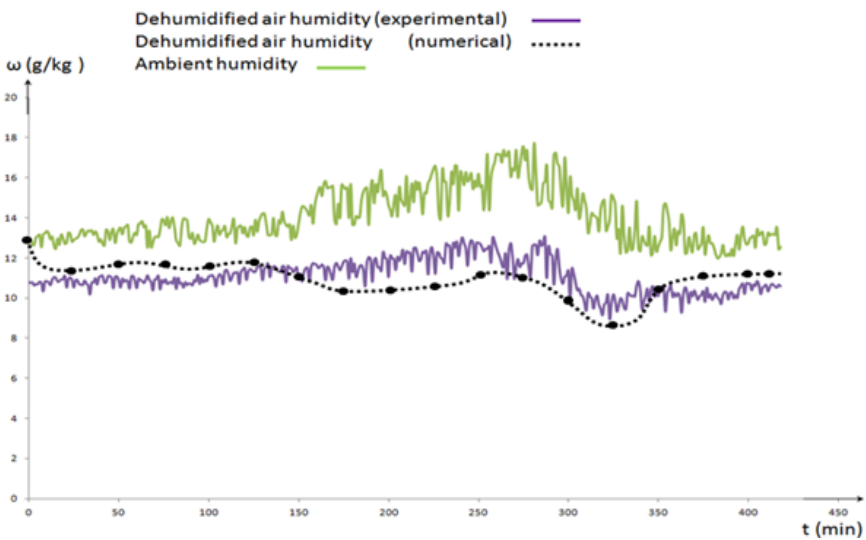


Fig. 7 Variation of numerical and experimental dehumidified air humidity

*B. Profiles of Air Temperature and Air Humidity Ratio in the Dehumidification Process*

Fig. 6 shows the variation of numerical and experimental dehumidified air temperature. The results show that the higher the temperature of the ambient air to dehumidify, the higher is the temperature gradient between the air to dehumidify and the dehumidified air. The numerical temperature gradient is between 0K and 14.4 K. Concerning the experimental gradient, it is between 2.9 K and 11.1 K.

Fig. 7 shows the variation of numerical and experimental dehumidified air humidity ratio. The results show that the higher the humidity ratio of the ambient air to dehumidify, the higher is the specific humidity gradient between the air to dehumidify and the dehumidified air. The numerical humidity

gradient is between 0 g/kg and 6.49 g/kg. Concerning the experimental gradient, it is between 1.84 g/kg and 5.83 g/kg.

*C. Profiles of Air Temperature and Air Humidity Ratio in the Regeneration Process*

Fig. 8 shows the variation of numerical and experimental rejected air temperature. The results show that the higher the regeneration temperature, the higher is the temperature gradient between the regeneration air and the rejected air. The numerical temperature gradient is between 0K and 22.6 K. Concerning the experimental gradient, it is between 7.14 K and 25.58 K.

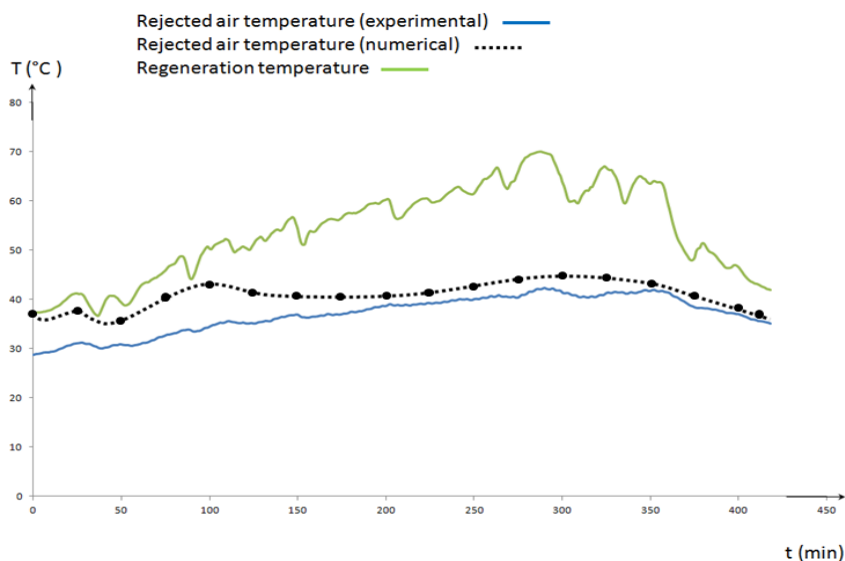


Fig. 8 Variation of numerical and experimental rejected air temperature

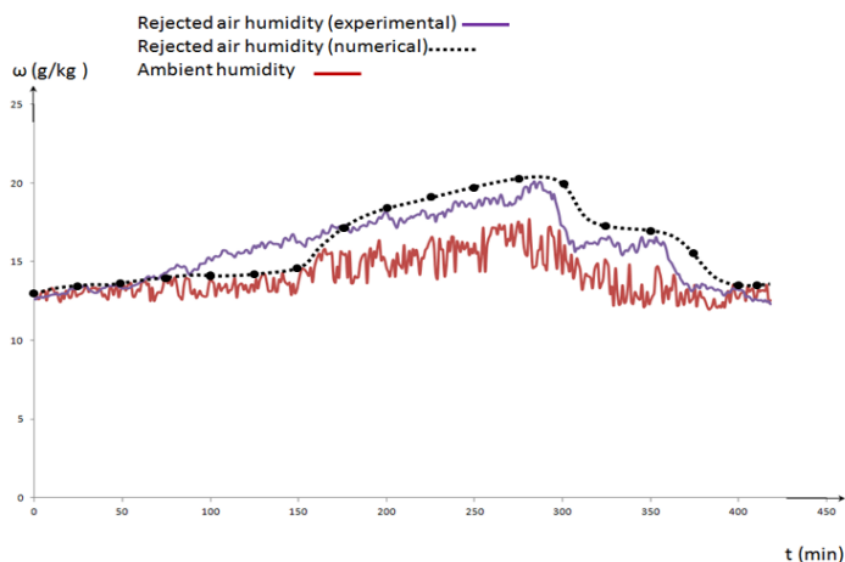


Fig. 9 Variation of numerical and experimental rejected air humidity

Fig. 9 shows the variation of numerical and experimental rejected air humidity ratio. The results show that the

regeneration phenomenon is effective only between 125 min and 360 min. Consequently, in real time between 11am 5min

and 3pm. This is due to the regeneration temperature which reaches an acceptable level to ensure the regeneration of the desiccant wheel in the same period of time. The numerical humidity gradient is between 0 g/kg and 5.75 g/kg. Concerning the experimental gradient, it is between “-0.61” g/kg and 3.76 g/kg.

As seen through the simulation study and the experimental investigation, a good agreement is found when comparing the model predictions with experimental data under the considered range of operating conditions. As a consequence, the developed model for the component key of the unit “the desiccant wheel” is validated.

## VI. COMPARTMENTS OF DESALINATION AND WATER CONDENSATION: NUMERICAL STUDY

### A. Compartment of Desalination

This study is based on the following calculation procedure (Fig. 10): The ambient air passes through the desiccant wheel to be dehumidified and heated from (T1, ω1) to (T2, ω2). Then, the dehumidified air is humidified close to the saturation in the humidifier HUM4 by the use of salty underground water from (T2, ω2) to (T3, ω3). Later on, this humidified air passes through a water/air heat exchanger HEX4 to be dehumidified by cooling under its dew point temperature from (T3, ω3) to (T4, ω4). As a consequence a quantity of pure water is obtained at the exit of the heat exchanger water/air HEX4.

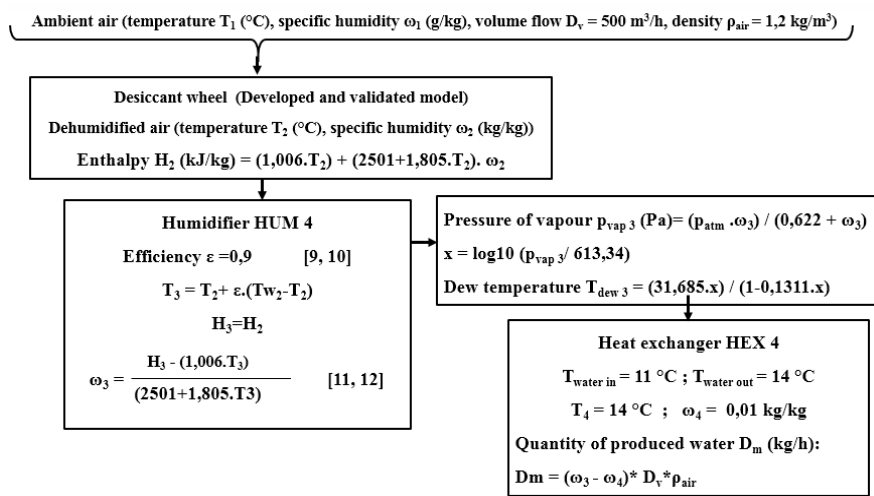


Fig. 10 Calculation procedure for the desalination compartment

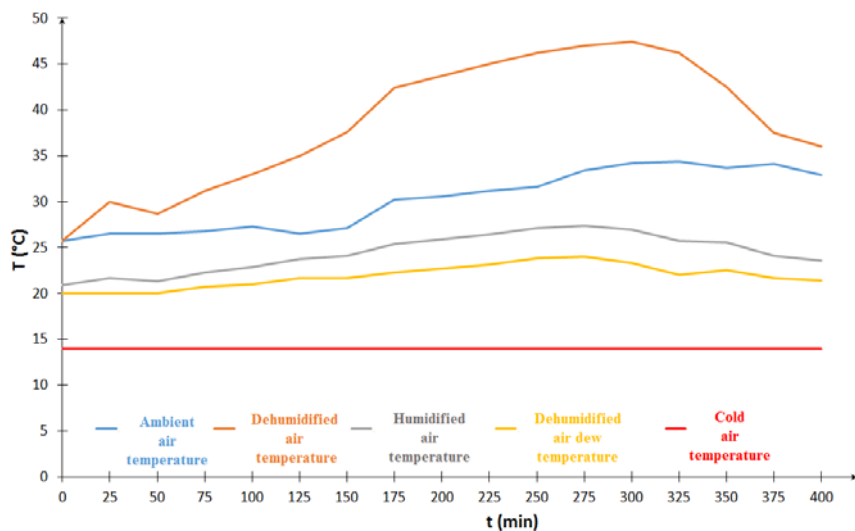


Fig. 11 Variation of air temperature in the desalination compartment

Fig. 11 shows the variation of air temperatures corresponding to every point of the compartment of desalination.

Fig. 12 shows the variation of air humidity corresponding to every point of the compartment of desalination.

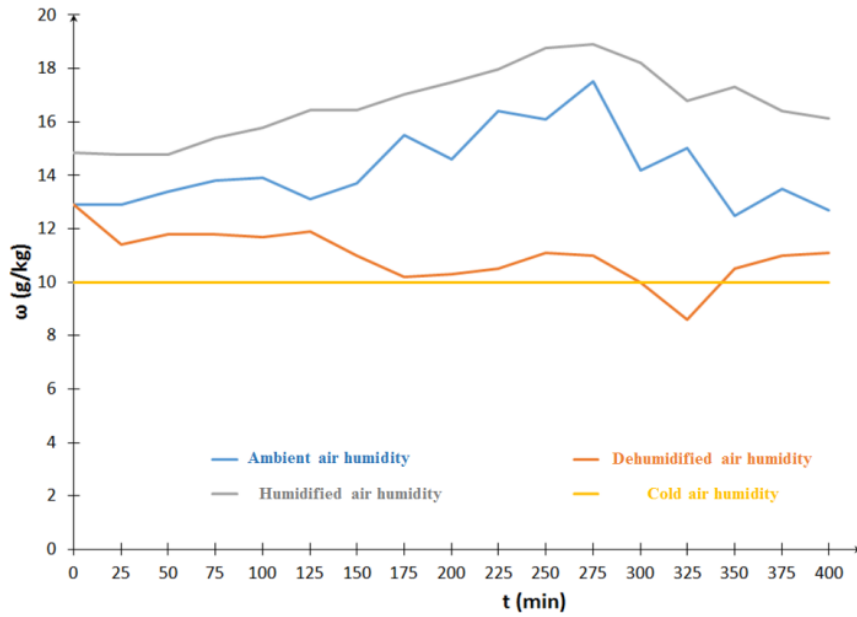


Fig. 12 Variation of air humidity in the desalination compartment

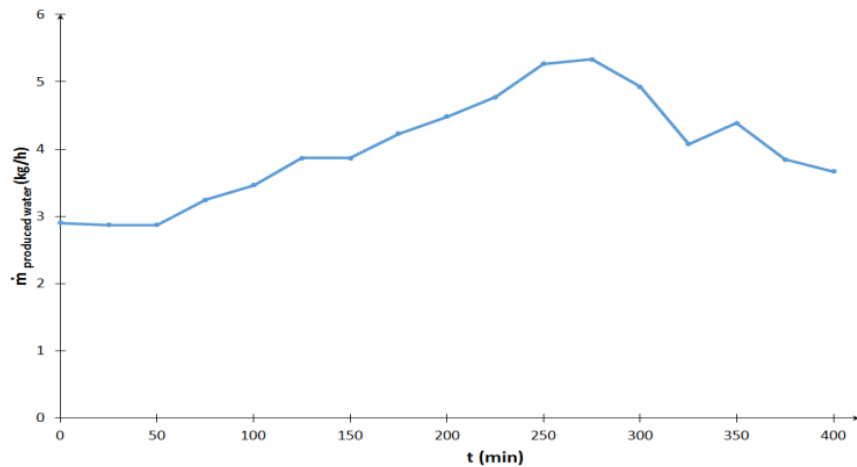


Fig. 13 Variation of mass flow of the obtained pure water in the desalination compartment

Fig. 13 shows the variation of mass flow of the obtained water at the exit of the heat exchanger HEX4. The results show that the variation of the mass flow is between 2.86 kg/h and 5.33 kg/h.

### B. Compartment of Water Condensation

This study is based on the following calculation procedure (Fig 14): The rejected air passes through the heat exchanger water/air HEX to be dehumidified by cooling under its dew point temperature from (T12, ω12) to (T13, ω13). As a consequence a quantity of pure water is obtained by condensation at the exit of the heat exchanger.

Fig. 15 shows the variation of air temperatures corresponding to every point of the compartment of water condensation.

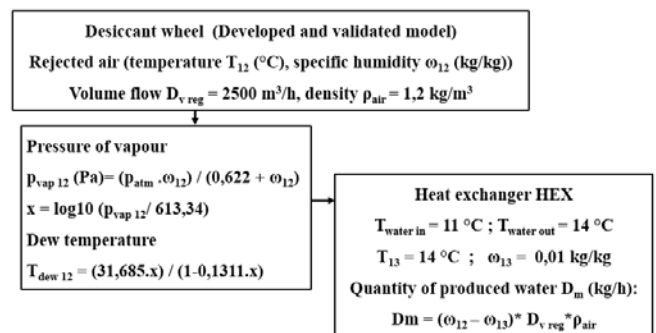


Fig. 14 Calculation procedure for the water condensation compartment



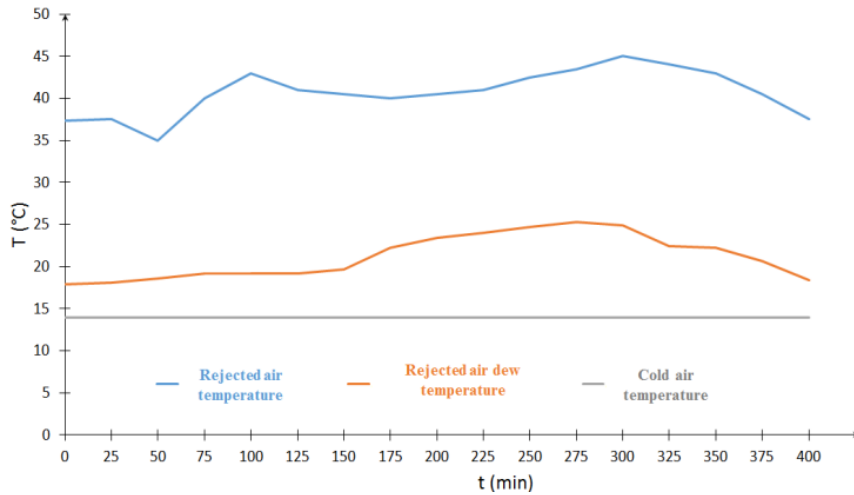


Fig. 15 Variation of air temperature in the water condensation compartment

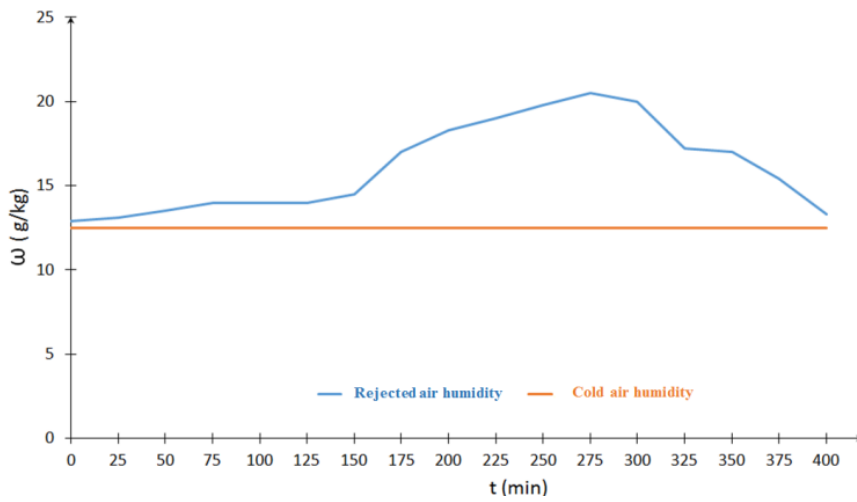


Fig. 16 Variation of air humidity in the water condensation compartment

Fig. 16 shows the variation of air humidity corresponding to every point of the compartment of water condensation.

water at the exit of the heat exchanger HEX. The results show that the variation of the mass flow is between 8.7 kg/h and 31.5 kg/h.

Fig. 17 shows the variation of mass flow of the obtained

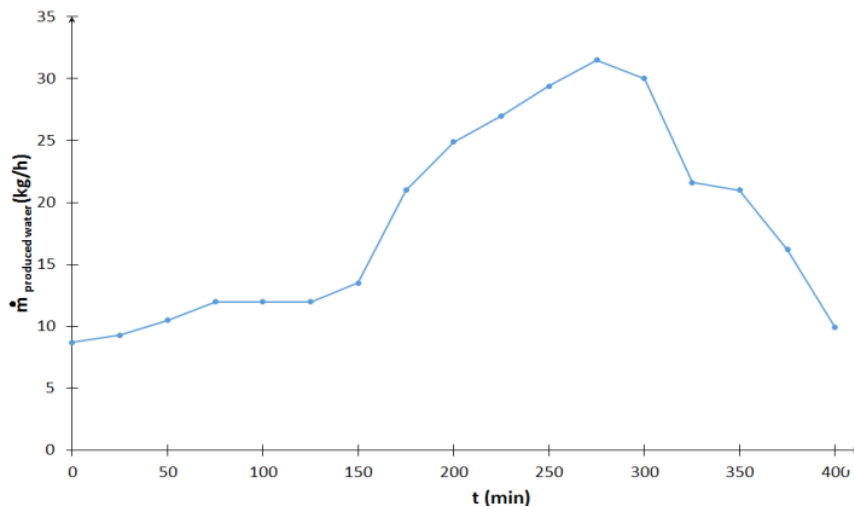


Fig. 17 Variation of mass flow of the obtained pure water in the water condensation compartment

## VII. CONCLUSION

A design of a new desiccant solar unit for air conditioning and desalination is developed. Furthermore, a modelling study is detailed for the desiccant wheel. As seen through the simulation study and the experimental investigation, the regeneration phenomenon can be done by use of relatively low temperature. Indeed this value does not exceed 70°C. This can be beneficial as it can facilitate the design of the regeneration stage. In addition, minimizing the value of the specific humidity and the value of the temperature of the air to dehumidify is very interesting. This can be beneficial as it facilitates the cooling of dehumidified air in desiccant solar air conditioning unit. Therefore, a pre-cooling stage before the dehumidification stage is interesting. This is done through the desalination compartment. In addition, this unit can produce water by desalination and water condensation from the rejected air and at the same time ensures the production of a conditioned air with taking into account thermal comfort conditions.

## REFERENCES

- [1] Y. J. Dai, R. Z. Wang, H. F. Zhang, J. D. Yu, Use of liquid desiccant cooling to improve the performance of vapour compression air conditioning, *Appl Therm Eng*, 21 (2001) 1185–1202.
- [2] P.L. Dhar, S.K. Singh, Studies on solid desiccant based hybrid air-conditioning systems, *Appl Therm Eng*, 21 (2001) 119-134.
- [3] Seiichi Yamaguchi, Jongsoo Jeong, Kiyoshi Saito, Hikoo Miyauchi, Masatoshi Harada, Hybrid liquid desiccant air-conditioning system: Experiments and simulations, *Appl Therm Eng*, 31 (2011) 3741-3747.
- [4] Sand JR, Fischer JC, Active desiccant integration with packaged rooftop HVAC equipment, *Appl Therm Eng*, 25 (2005) 3138-3148.
- [5] Hans-Marting Henning, Solar assisted air conditioning of buildings – an overview, *Appl Therm Eng*, 27(2007) 1734–1749
- [6] Chaouki Ali; Habib Ben Bacha; Mounir Baccar; Aref Y. Maalej, Dynamic modelling and simulation of a new air conditioning prototype by solar energy, *Renewable Energy*, 32 (2007) 200-215.
- [7] G. Panaras, E. Mathioulakis, V. Belessiotis, Solid desiccant air conditioning systems -Design parameters, *Energy*, 36 (2011) 2399-2406.
- [8] Zied Guidara, Wissem Zghal, Habib Ben Bacha, Modelling and simulation study of regeneration and dehumidification stages used in solar air conditioning unit, *International Journal of Mechanics and Energy*, Vol. 1, Issue 1, (2013) 54-64.